Environmental Pollution 315 (2022) 120480

Contents lists available at ScienceDirect

Environmental Pollution

journal homepage: www.elsevier.com/locate/envpol

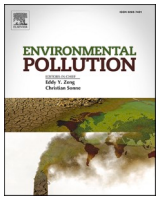

Polystyrene microplastic ingestion induces the damage in digestive gland of *Amphioctopus fangsiao* at the physiological, inflammatory, metabolome and transcriptomic levels☆

Jian Zheng [a,b], Congjun Li [c], Xiaodong Zheng [a,b,*]

[a] Institute of Evolution & Marine Biodiversity (IEMB), Ocean University of China, Qingdao, 266003, China
[b] Key Laboratory of Mariculture, Ministry of Education, Ocean University of China, Qingdao, 266003, China
[c] Laboratory of Marine Protozoan Biodiversity and Evolution, Marine College, Shandong University, Weihai, 264209, China

ARTICLE INFO

Keywords:
Polystyrene microplastics
Histopathological damage
Amphioctopus fangsiao
Toxic effects
Detoxification

ABSTRACT

Microplastics are ubiquitous in the aquatic and terrestrial ecosystem, increasingly becoming a serious concern for aquatic organism health. However, information regarding the effects of microplastics on cephalopods is remain limited to date. *Amphioctopus fangsiao*, an important economic species in cephalopods, can serve as a potential indicator of environmental pollution due to its short life expectancy and high metabolic rates. Here, to explore the toxic effects during the microplastic stress response, we analyzed the growth performance, histopathological damage, oxidative stress biomarkers, metabolomic and transcriptomic response in digestive gland of *A. fangsiao* under different concentrations (0, 100 and 1000 μg/L) of commercial polystyrene microplastics (MPS) exposure (5 μm, sphere) for 21 days. The results showed that MPS exerted a huge influence on the growth performance of *A. fangsiao*. The oxidative stress and inflammation in digestive gland of *A. fangsiao* were also detected after exposure to MPS. In addition, most of the altered metabolites observed in the metabolic analysis were related to inflammation, oxidative stress and glucolipid metabolism. Transcriptome analysis detected the differentially expressed genes (DEGs) and the significantly enriched KEGG pathways associated with glycolipid metabolism, inflammation and DNA damage. Collectively, our results indicate that excessive environmental microplastic exposure will cause toxicity damage and then initiate the detoxification mechanism in *A. fangsiao* digestive gland to maintain homeostasis. This study revealed that microplastic can cause adverse consequences on cephalopods, providing novel insights into the toxicological effect of microplastic exposure.

1. Introduction

Global plastic production has risen sharply because of the widespread use of plastic materials in recent years (Janajreh et al., 2015). According to statistics, plastic production has rapidly increased to 367 million tons in 2021 (Plastics Europe, 2022). Microplastics are produced by the degradation of plastic products, which are 1–5000 μm in size. The sources of microplastics can be divided into the following two pathways. The microplastic additives produced directly and used in daily necessities (like face wash and cosmetics) are called primary microplastics. Whereas the tiny particles decomposed through biological, chemical and physical processes, such as acrylic clothing and nylon, are considered as secondary microplastics (Peters and Bratton, 2016).

Microplastics are found in various systems, including inland rivers, seawater, and even in polar regions (Kuhn and van Franeker, 2020; Xu et al., 2020; Mishra et al., 2021). Polystyrene (PS) is mainly derived from personal care products, which can accumulate in large quantities in the livers and intestines of marine organisms (Browne et al., 2008; Ding et al., 2018). Increasing evidence has shown that gene expression (Zhao et al., 2020; Xiang et al., 2022), energy and lipid metabolism (Wan et al., 2019), oxidative stress (Wan et al., 2019), inflammatory response (Lu et al., 2016; Wan et al., 2019), physiological behavior (Lu et al., 2016), reproduction (Sussarellu et al., 2016) and morphology (Xiang et al., 2022) of aquatic life have been affected by PS exposure.

Cephalopoda is the third-largest class in Mollusca (Lindgren et al., 2004; Xu, 2008). It has over 800 identified species, of which some

☆ This paper has been recommended for acceptance by Maria Cristina Fossi.

* Corresponding author. Institute of Evolution & Marine Biodiversity (IEMB), Ocean University of China, Qingdao, 266003, China.
E-mail address: xdzheng@ouc.edu.cn (X. Zheng).

https://doi.org/10.1016/j.envpol.2022.120480
Received 31 August 2022; Received in revised form 10 October 2022; Accepted 17 October 2022
Available online 20 October 2022

species are promising species for mariculture due to their long history of utilization of food and medicine (Lu, 2000). Recently, microplastics have been found in the tissues of many cephalopods. Microplastics with different shapes, colors and polymer types have been found in many cephalopods, such as *Vampyroteuthis infernalis* (Ferreira et al., 2022), *Abralia veranyi* (Ferreira et al., 2022), *Octopus vulgaris* (Pedà et al., 2022), *Dosidicus gigas* (Gong et al., 2021) and *Sepia officinalis* (Oliveira et al., 2020) and. However, the toxicological effect of microplastic on cephalopods is still unexplored.

Amphioctopus fangsiao, is also known as the synonym name of *Octopus ocellatus*, which is one of the most representative cephalopods (Jiang et al., 2020). For the following reasons, it has the potential to indicate the level of local environmental pollution. Firstly, it has territorial nature and small-scale activity areas, which allows them to reflect their local habitat environmental quality (Mangold, 1983; Bu et al., 2021). Secondly, it has a relatively short life expectancy (about one year), which can be mainly divided into embryonic phase (about one month), juvenile phase (about three months), sub-adult phase (about four months) and adult phase (about four months) (Vidal et al., 2014; Wang et al., 2015; Jiang et al., 2020; Ibáñez et al., 2021). This characteristic causes the high metabolic rates and growth rates of *A. fangsiao*. Therefore, pollutants may be accumulated rapidly in their bodies (Wang et al., 2015; Bu et al., 2021). Finally, *A. fangsiao* is widely distributed across the Pacific Northwest, where high concentrations of microplastics have been detected. For example, the abundance of microplastics along Qingdao coast in the Yellow Sea was 567.50 ± 101.06 items/m^3 (Gao et al., 2021); Eo et al. (2018) reported that there was also a high abundance of microplastics along the Korean coast (1400–65,000 items m^2). As a generalist predator, *A. fangsiao* is more likely to accumulate pollutants from the prey (García et al., 2002). Here, a total of 54 *A. fangsiao* were used to perform this experiment of polystyrene microplastic (MPS) exposure. The aims of this study are thus to test if the ingestion of MPS affects the growth performance and digestive gland function of *A. fangsiao*. The results of this study, including histopathological damage, oxidative stress, metabolic disorders and transcriptional responses, offer a novel insight into the response mechanism of the octopus under microplastic exposure.

2. Materials and methods

2.1. Experimental animals, polystyrene microplastics, and exposure treatment

Fifty-four sub-adult *A. fangsiao* (about 200 days of age, mantle length: 65.15 ± 13.35 mm, weight: 57.145 ± 21.839 g) (supplemental Table. S1), were sampled from Jiaxin Aquaculture Farm, China. All individuals were reared at laboratory for 7 days to acclimatize with >6.5 mg/L of dissolved oxygen, 7.9–8.2 of PH, 17–18 C of temperature and 32‰ of salinity. *A. fangsiao* individuals were farmed in eighteen experimental tanks (60-L, 3 octopuses per tank). Then, they were provided with enough *Ruditapes philippinarum* for food every morning (5 individuals per octopus). A third of the seawater was replaced every day in all tanks.

Polystyrene sphere (PS) with a diameter of 5 μm used in this experiment was purchased from Tianjin BaseLine ChromTech Research Centre (Tianjin, China). This size of PS has been observed extensively in aquatic environments (Eerkes-Medrano et al., 2015; Zhao et al., 2020). In addition, previous studies have found that 5 μm of PS was more likely to accumulate in aquatic organisms compared with it in 70 nm and 20 μm (Lu et al., 2016; Qiao et al., 2019). Therefore, 5 μm PS was used in this study. The emission scanning electron microscope was used to observe the shape and size (ZEISS merlin compact 61–78, Germany) (supplemental Fig. S1A). The chemical component of PS was characterized by Fourier transform infrared (FTIR) spectroscopy (Thermo Fisher IS50, USA) (supplemental Fig. S1B). The absorption peaks were basically consistent with previous studies, confirming the microplastic used in this study is polystyrene (Lu et al., 2016; Qiao et al., 2019).

The stock suspension of MPS was prepared as described by Teng et al. (2021a) and the different concentrations of microplastic solutions were prepared by weighing the remaining particles after evaporating the water as described by Xiang et al. (2022). The concentrations of MPS in this study were 0 μg/L, 100 μg/L and 1000 μg/L. The lower concentration would presumably represent the realistic conditions of the seabed where the *A. fangsiao* lives. While the higher concentration has a stronger effect on *A. fangsiao*, and the adaptive mechanism from physiological to molecular responses is easier to analyze. The larger toxicological effect can arouse more attention to the protection of marine environment. In addition, many studies have shown that these concentrations of microplastic have a huge adverse effect on aquatic life (Wan et al., 2019; Zhao et al., 2020; Teng et al., 2021a; Teng et al., 2021b; Xiang et al., 2022).

Control group (Control, 0 μg/L), low-concentration of MPS group (PS-L, 100 μg/L) and high-concentration of MPS group (PS–H, 1000 μg/L) were set up. To keep the water clean, a third of the seawater of all tanks was replaced every day and the corresponding MPS solution was added. All other culturing conditions were consistent with those during acclimatizer.

2.2. Effects of MPS on the growth of A. fangsiao

After 21-days exposure, a total of 18 (6 per group) *A. fangsiao* was euthanized with an overdose of anesthetic, and measured for the weight of the body and digestive gland (precision 0.001 g). The following equations were used to measure the growth performance of *A. fangsiao*:

$$SGR = \frac{[\ln W_f - \ln W_i]}{T};$$

$$HIS = W_d \,/\, W_f \times 100.$$

where SGR is the specific growth rate, W_f is the weight of the final body after MPS exposure, W_i is the weight of the initial body, HIS is the hepatosomatic index, and W_d is the weight of the final digestive gland after MPS exposure.

2.3. Biochemical indicator analysis

For the determination of biomarkers, 1 g of the digestive gland tissues from three freshly killed *A. fangsiao* per group was collected. And then these tissues were homogenized in PBS (5 ml, pH7.5) which included the protease inhibitors by a sonicator. The homogenates were centrifuged for 15 min (5000 g, 4 °C). Subsequently, the supernatants were collected. The protein concentrations were detected by BCA Protein Assay Kit (CoWin Biosciences, China, article number: CW00145). Based on the methods described by Okutan et al. (2005), the protein level was measured by commercial kits (Beyotime, China), including reactive oxygen species content (ROS, article number: S0033S), lipid peroxidation's level (malondialdehyde, MDA content) (article number: S0131S), superoxide dismutase (SOD, article number: S0086) and catalase (CAT, article number: S0082) activities. In addition, the commercial kits from Nanjing Jiancheng Bioengineering Institute (Nanjing, China) were used to analyze the glycolipid metabolism responses, glucose, (Glu, article number: F006-1-1); pyruvic acid (Pyr, article number: A081); total cholesterol (T-CHO, article number: A111-1-1); triglyceride (TG, article number: A110-1-1)) in digestive glands. The details can be found in the kit manufacturers' instructions.

2.4. Integrated biomarker response (IBR) analysis

IBR analysis is a method to assess the effects of external pressure on living organisms. IBR version 2 described by Sanchez et al. (2013) was used to assess the comprehensive effects of MPS on *A. fangsiao*. Firstly,

the data of biochemical indicators in treatment groups (X_i) were compared to these data in the control group (X_0). To reduce variance, log transformation was carried out. The equation is as follows: $Y_i = \log\text{-}X_i/X_0$. The next step was to calculate the standard deviation (s) and the general mean (m) of Y_i and then Y_i was standardized according to the equation ($Z_i = Y_i\text{-}m)/s$. Subsequently, the biomarker deviation index (A) was calculated based on equation $A = Z_i\text{-}Z_0$, where Z_0 is the standardized biomarker in the control group. Finally, the equation IBR value $= \Sigma|A|$ was used to calculate IBR values. Besides, the biomarker deviation index (A) of single biomarker was also used to draw the star plot. The biomarker induction was reflected by the area above 0, and the biomarker inhibition was indicated by the area below 0.

2.5. Histological analysis

A total of 18 *A. fangsiao* (6 individuals in each group) were used to measure the damage of digestive gland. Bouin's fixative was used to fix the digestive gland tissues for 24 h. And then these tissues were sectioned at 5 μm-thickness after embedding in paraffin wax. After deparaffinizing and rehydrating, the slides were stained by hematoxylin-eosin (HE) (Beyotime, China, article number: C0105S). Finally, the slides were observed using an Olympus BX53 fluorescent microscope (Olympus, Japan).

2.6. Effect of MPS exposure on the digestive gland transcriptome

After the 21-day exposure experiment, six *A. fangsiao* individuals (three from the control group and PS-H group, respectively) were sampled after the anesthesia with the overdose of anesthetic ($MgCl_2$, 7%). The 50 mg digestive glands were then dissected out of the octopuses and frozen ground in 800 ml RNAiso plus (TaKaRa) at −80 °C till use. Total RNA was extracted by commercial kits TRIzol reagent (Takara Biochemicals). The samples satisfying the requirement (OD260/230 ≥ 2.1, OD260/280: 1.9–2.0, 28/18 S ≥ 1.0, >50 μg) were sent to the Biomarker Technologies Co. Ltd., Beijing, China to construct the library. The process is as follows. The mRNA was isolated by the magnetic beads with Oligo (dT) and randomly fragmented by Fragmentation Buffer. The cDNA was then purified using fragmented mRNA as the template and amplified by PCR to obtain cDNA library. Qubit 2.0 and Agilent 2100 were used to examine the library and the qualified library was sequenced on the Illumina sequencing platform.

Filtered sequencing clean data was stored in FASTQ format file using FASTP software (Chen et al., 2018). HISAT2 software was used to map this data to the genome sequence of *A. fangsiao* (unpublished data) (Kim et al., 2015).

The gene functions were annotated based on Gene Ontology (Go), NCBI non-redundant protein sequences (Nr) and Kyoto Encyclopaedia of Genes and Genomes database (KEGG) by HMMER3, BLAST2GO (https://www.blast2go.com/) and KOBAS (Conesa et al., 2005; Kanehisa et al., 2007; Bu et al., 2021). Besides, the principal component analysis (PCA) was performed by GCTA software (Yang et al., 2011). To reflect sample variation, the first three significant components were detected and the significance of the principal components was examined by the Tracy–Widom test (Zheng et al., 2022). The accession number of the sequencing data in the NCBI Sequence Read Archive database was SRR21871815-SRR21871820.

DEseq2 software was used to determine the differential expression genes (DEGs) (Love et al., 2014), and *q*-value was set up as filtering thresholds. KEGG pathways were enriched based on these DEGs, and these pathways with *q*-value ≤ 0.05 were used as significant enrichment.

2.7. Validation of significant genes

To validate significant genes detected in transcriptome analysis, eight DEGs were chosen for qRT-PCR analysis. *GAPDH* and *β-actin* genes were used as reference genes. Supplemental Table S2 shows primer sequences amplified DEGs and reference genes. The total RNA identical to the transcriptome analysis was used in the qRT-PCR analysis. The recombinant DNase I (TaKaRa, Japan) and the reverse transcription kit (TaKaRa, Japan) were used to synthesize the first-strand cDNAs. The reaction system was performed as described by Li et al. (2022). Triplicates were performed to reduce technical errors. The comparative C_t ($2^{-\Delta\Delta Ct}$) method was used to calculate the relative expression of all DEGs (Zhao et al., 2021).

2.8. /MS nontargeted metabolomic analysis

The metabonomic analysis is a method to identify metabolites with significant differences and important biological significance. The digestive gland tissue of 12 *A. fangsiao* (6 from the control group, 6 from the PS-H group, and duplicate individuals with growth performance measurement) was used to perform metabolomic analysis following standard procedures described by Teng et al. (2021a).

The identified compounds were searched for classification and pathway information in KEGG, human metabolome database (HMDB) and lipid maps proteome database (LMPD). T-test was used to analyze the different significance *p*-value of each compound based on the different multiples. The R language package "ropls" was used to perform Orthogonal Partial Least Squares-Discriminant Analysis (OPLS-DA), and 200 times permutation tests were performed to verify the reliability of the model. The method of combining the difference multiple, the *p*-value and the VIP value of the OPLS-DA model were adopted to screen the differential metabolites. The screening criteria were Fold change > *p*-value < 0.05 and VIP >1. KEGG pathways were enriched based on these differential metabolites, and these pathways with *q*-value ≤ 0.05 were used as significant enrichment.

3. Result and discussion

3.1. Effects of MPS exposure on the growth performance of A. fangsiao

Fig. 1 Showed the growth performance of *A. fangsiao* after 3-week of rearing. No remarkable differences in specific growth rate were found for both the PS-L and control groups after 21 days of exposure, while a significant reduction ($p < 0.01$) was seen in the PS-H group. Besides, the hepatosomatic index declined significantly ($p < 0.05$, $p < 0.001$) in the PS-L and PS-H groups.

These results suggested that MPS exposure has restrained growth and energy conversion. Previous researches have reported the microplastic accumulation of aquatic organism in the gut, digestive glands, gill and skin (Feng et al., 2019; Liu et al., 2019; Zhao et al., 2020), showing that these particles can be ingested and absorbed through the digestive system. And the smaller size of microplastics could have a greater toxicological effect on aquatic organisms (Browne et al., 2008). Microplastic ingestion caused the malabsorption of *A. fangsiao*, which reduced food

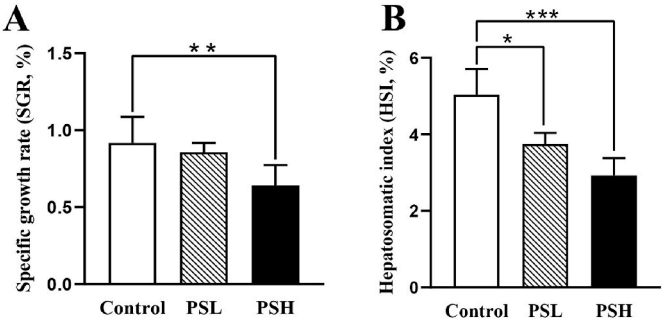

Fig. 1. Specific growth rate (SGR) (**A**) and hepatosomatic index (HIS) (**B**) in different treatments. Data indicate mean ± S. D. (n = 6). ***$p < 0.001$, **$p < 0.01$, *$p < 0.05$.

intake and conversion. The data were supported by the biochemical indicator activity of lipid metabolism (see below). Similar results in other aquatic life were also confirmed (Lucia et al., 2010; Liu et al., 2019; Chen et al., 2020). However, some studies have shown that microplastic exposure has no obvious adverse effects on the growth performance of several invertebrates, such as *Crassostrea gigas* and *Gammarus pulex* (Cole and Galloway, 2015; Weber et al., 2018). One possible reason is the differences in adaptation of species, microplastic characteristics (additives, shape, size and type), and exposure patterns (microplastic concentration, duration). Overall, these results revealed that 5 μm MPS exposure inhibited the growth of *A. fangsiao*.

3.2. Effects of MPS exposure on oxidative stress, lipid peroxidation and glucolipid metabolism

3.2.1. Oxidative stress markers

Several biochemical indicators were analyzed to measure the level of oxidative stress and lipid peroxidation. ROS levels were shown in Fig. 2A. ROS level is one of the most commonly used biomarkers of environmental pollution exposure (Avio et al., 2015a). In the PS-H group, the mean value of ROS content has a distinct increase ($p < 0.005$), indicating that MPS exposure elicited a rise in ROS levels in the digestive gland. The MDA content has also markedly increased in the PS-H group ($p < 0.05$). The level of lipid peroxidation showed an obvious rising remarkably in response to increasing MPS concentration (Fig. 2B). Likewise, in the PS-L and PS-H treated octopuses, the enzyme activity of SOD and CAT in the digestive gland was significantly higher than those in the control group ($p < 0.05$, $p < 0.01$; Fig. 2C and D). These results uncovered that the negative effects were found in terms of oxidative stress parameters including ROS and MDA for treatment with MPS, thereby evoking the imbalance of homeostasis. And SOD and CAT, as the antioxidant enzymes, were both produced to protect the cells from the oxidative damage caused by MPS stress in digestive glands.

The above findings exhibited that MPS exposure affected oxidative stress response of digestive gland cells in a concentration-dependent manner. ROS are the by-products of oxidative phosphorylation, and the essence of oxidative stress is the imbalance in the generation and detoxification of ROS (Li et al., 2022). ROS can damage cellular functionality and integrity by reacting with cell components (such as lipid and protein) (Li et al., 2022). We found a considerable increase in intracellular ROS levels for all concentrations tested, suggesting the strong oxidative damage of digestive gland cells caused by excessive ROS under MPS stress (Paul-Pont et al., 2016). Due to the overload of ROS, MDA content represented the level of lipid peroxidation showed an obvious response to the high level of MPS exposure with a significant rising in the digestive gland. With the chronic damage caused by oxidative stress, the enzyme activity of SOD was enhanced to assist with tolerating elevated MPS levels in digestive gland. Similar results were found in the *C. gigas* exposed to polyethylene terephthalate (Teng et al., 2021b) and in *Mytilus edulis* exposed to MPS (Paul-Pont et al., 2016). Besides, as past work suggests CAT plays a critical role in coping with exogenous hydrogen peroxide (Avio et al., 2015b). Similarly, the activity of CAT was stimulated in the digestive glands following exposure to MPS, further indicating the apparent antioxidant defense mechanism

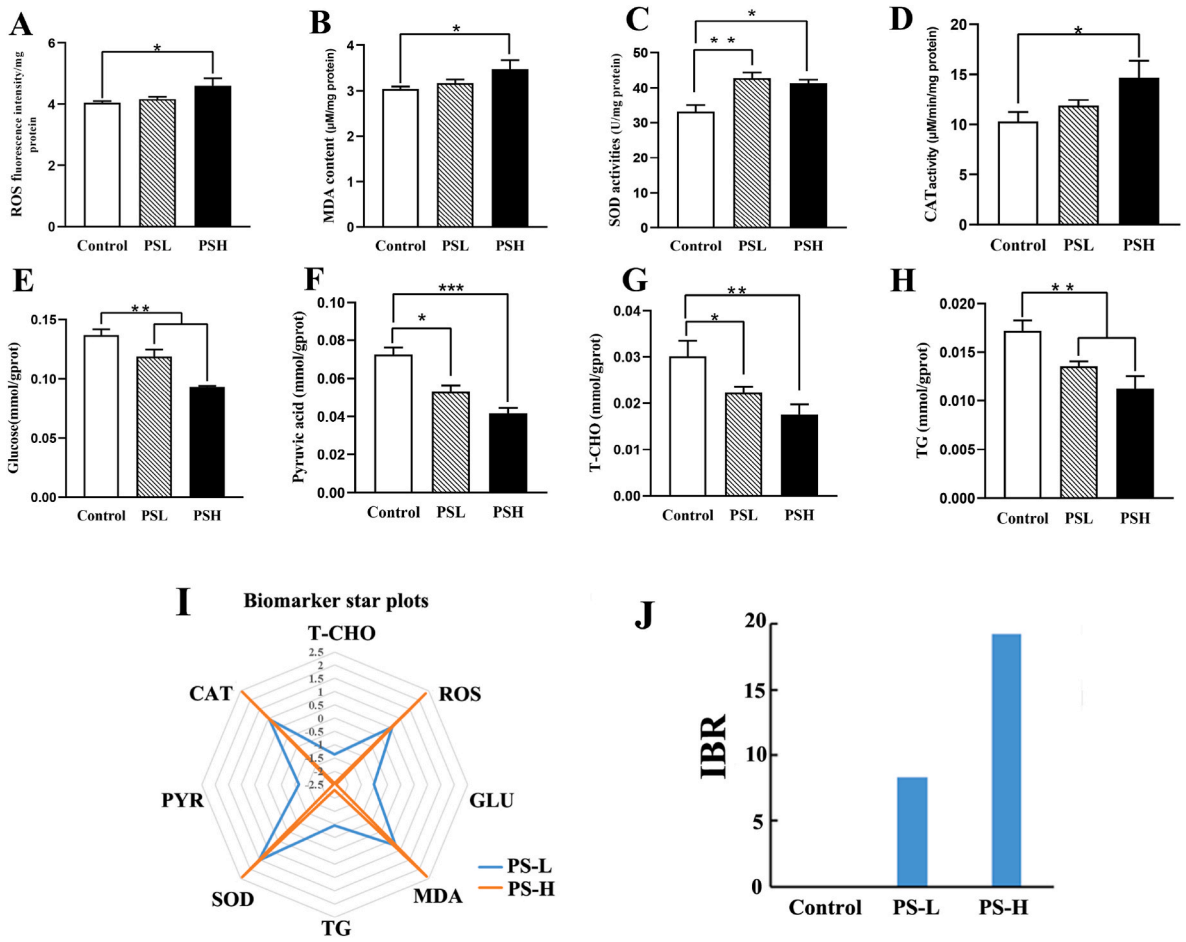

Fig. 2. The ROS level (**A**), MDA content (**B**), SOD activity (**C**) and CAT activity (**D**), and the changes in glucolipid metabolism responses (**E-H**) in the digestive glands of *A. fangsiao* under MPS stress. Biomarker star plots in the digestive glands of *A. fangsiao* following 21 days of exposure to MPS (**I**). Calculated IBR index utilizing the biochemical parameters following 21 days of exposure to MPS (**J**). Data indicate mean ± S. D. (n = 3). ***$p < 0.001$, **$p < 0.01$, *$p < 0.05$.

of *A. fangsiao* to defend against microplastic toxicity. To conclude, our data showed that MPS stress caused an increase in ROS level, and translated into an elevation in lipid peroxidation and the activation of CAT and SOD, involved in response to oxidative stress.

3.2.2. Glucolipid metabolism markers

In this study, the levels of Glu and Pyr, T-CHO and TG were analyzed to assess the glucolipid metabolism alteration in the digestive gland. Glu and Pyr, both of which were key components in glycolysis, have significantly declined following the exposure to MPS (Fig. 2E and F). Likewise, the T-CHO and TG contents associated with lipid metabolism were observed a similar decrease trend (Fig. 2G and H).

Our results demonstrated that MPS stress would induce glucolipid metabolism alteration. In the glycolytic pathway, Glu and Pyr are the precursor and product, respectively (Zhao et al., 2020). The decline in glucose and pyruvic acid suggested that MPS exposure could induce the alteration of glucose metabolism in the digestive glands, which was consistent with other aquatic life previously observed, such as zebrafish (Lu et al., 2016) and oysters (Teng et al., 2021a). MPS can cause physical injury to aquatic organisms by blocking the digestive tract and preventing enzyme production, which may be the cause of metabolic alteration in digestive glands of *A. fangsiao* (Xiang et al., 2022). Moreover, glucose metabolism alteration also could affect the subsequent stages of the ATP obtention (TCA cycle and oxidative phosphorylation) because of a lower input of fuel, causing the alteration of free radicals from the cell metabolism (Pan et al., 2018), which is also confirmed by the findings of oxidative stress. The decrease of the ATP can also result in energy shortage of *A. fangsiao*, thereby reducing their growth performance.

As the primary components of lipids, triglyceride (TG) and total cholesterol (T-CHO) can produce energy by hydrolysis or oxidation reaction, both of which are crucial energy reserves and sources (Prato et al., 2010; Martínez-Pita et al., 2012; Filimonova et al., 2016). Here, TG and T-CHO levels were decreased with the increasing MPS concentration, indicating that MPS exposure was significantly detrimental to lipid metabolism in digestive glands tissues. The TG decrease may reflect the activation of the lipid oxidation to obtain acetyl-CoA and continue the ATP obtention, implying the problems of nutrition and energy of *A. fangsiao* (Zhao et al., 2020). The TG and T-CHO levels are closely related to the membrane structure of cells (Brandts et al., 2021). The decline in TG and T-CHO reflected a change related to membrane integrity to increase phospholipid production, suggesting possible membrane damage results from MPS exposure (Zhao et al., 2020; Brandts et al., 2021). The increase in MDA in the high concentration of MPS exposure also supported this result. Besides, the DEGs (such as Pyruvate dehydrogenase kinase and Peroxisome proliferators activated receptors-α) and differential metabolites (such as Glucosyl passifloate) associated with glucolipid metabolism were also found and varied by transcriptome and metabolome analysis, which further supported the above results.

3.2.3. IBR analysis

To assess comprehensively the toxicological effect of environmental stress on *A. fangsiao*, IBR index was analyzed in our paper. The above biomarkers responses for all concentrations tested are shown in star plots (Fig. 2I). In addition, the IBR index exhibited concentration-dependent following the exposure to MPS (Fig. 2J).

IBR analysis is an effective ecological method based on the response of biomarkers to environmental pollutants. It can be used to assess the toxical sensitivity in tested aquatic life (Lin et al., 2014). The varying area of star plots showed that there was a huge effect of MPS exposure on *A. fangsiao*. High IBR values increasing with MPS concentration tend to reveal increased toxic effects in the digestive gland of *A. fangsiao*.

3.3. Effects of MPS exposure on histology

Representative histological maps from three groups were shown in Fig. 3. Significant histopathological damages were found in the treatment groups. Necrosis, vacuolation and infiltration were observed in digestive gland tissue in groups treated with PS. This result revealed early inflammatory responses of *A. fangsiao* on PS exposure.

Previous works have investigated that the digestive gland is one of the most critical target organs for microplastics, but similar results in octopuses have not been detected previously (Lu et al., 2016; Zhao et al., 2020). To cope with the effects of microplastics, the first defense strategy of the digestive gland, including vacuolation and infiltration, was stimulated (Rochman et al., 2014). Consecutively, necrosis of digestive gland cells appeared in large numbers. The severity of damage within the digestive gland cells increases with the MPS concentration. The main reasons for this result may be the mechanical abrasion of microplastics to the digestive gland and the toxicological effect of chemical additives released by microplastics (Jabeen et al., 2018; Zhao et al., 2020).

3.4. Effects of MPS exposure on transcriptomic profiles

To assess the effect of *A. fangsiao* digestive gland under MPS exposure at a molecular level, 6 octopuses (3 from the PS-H group and 3 from the control group) were utilized to carry out the comparative transcriptome analysis. A total of 38.21 G of clean data were generated. As shown in PCA analysis (Fig. 4A), the biological replicates within the group were close to each other but far from the other groups, revealing the reproducibility and reliability of RNA-seq data. A total of 542 DEGs were obtained between groups (322 up- and 220 down-regulated) (Fig. 4B). The heatmap was illustrated to show the expression of DEGs in all groups (Fig. 4C).

The KEGG enrichment analysis of the differentially expressed genes suggested that these DEGs may play a role in various pathways. The supplemental Fig. S2 showed the top 20 pathways, which mainly involved in genetic information processes (mismatch repair, DNA replication), nucleotide metabolism (pyrimidine metabolism), replication and repair (base excision repair), amino acid metabolism (tyrosine, tryptophan and phenylalanine biosynthesis) and so on.

Significant DEGs and KEGG pathways involved in DNA damage, transmembrane transport, glucolipid metabolism and oxidative stress were detected by transcriptome analysis, and eight of these DEGs were examined for qRT-PCR (Fig. 5, supplemental Table S2). The qRT-PCR results uncovered consistent expression patterns with transcriptome analysis, verifying the accurate and reliable results of comparative transcriptome analysis (supplemental Fig. S3).

The rate-limiting enzyme DEGs associated with glucose metabolism were found at the transcript level, such as Pyruvate dehydrogenase kinase (PDK). In the glycolytic pathway, Pyruvate converted from glucose is rapidly converted to acetyl-CoA in mitochondria by PDK. The acetyl-CoA is then oxidized to obtain energy (Xiang et al., 2022). The lipogenesis can be regulated by Peroxisome proliferators-activated receptors (PPARs) family (Zhao et al., 2020). The suppression of PPAR-α gene was observed, confirming the disturbance of lipid metabolism.

The adverse effects of peroxide and superoxide overproduction can be amplified by iron overload under inflammatory conditions (Tisma et al., 2009). In cells, therefore, ferritin can participate in oxidative reactions by restricting the availability of iron (Tisma et al., 2009). In this study, the downregulation of ferritin gene verified the damaging effect of MPS exposure on oxidative stress. The free iron was excessively generated in digestive gland cells under MPS exposure conditions by proteolysis of ferritin, resulting in oxidative damage of *A. fangsiao* (Tisma et al., 2009). Besides, aquaporin is a membrane channel proteins family, which exerts a crucial role in facilitating the transport of certain neutral solutes and water (Bienert et al., 2007). In recent years, however, many studies have reported that aquaporins can transport ROS and NO, which played a critical role in antioxidant action and the

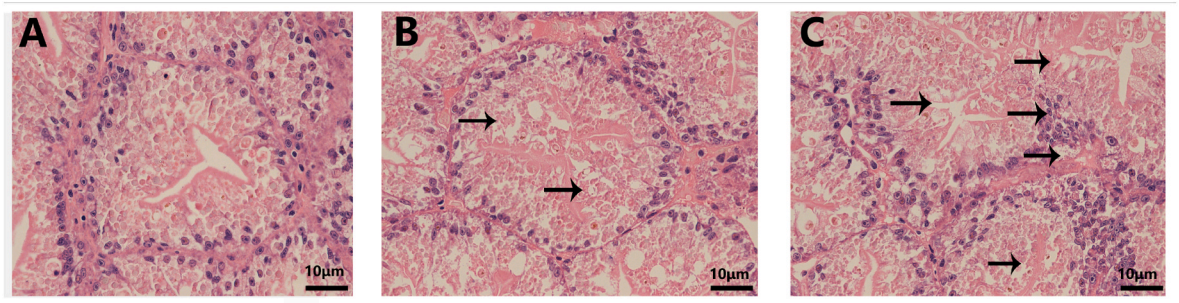

Fig. 3. Micrographs of digestive gland in the control group (**A**), PS-L group (**B**) and PS-H group (**C**) following 21 days of exposure to MPS. The histopathological damages are shown by black arrows.

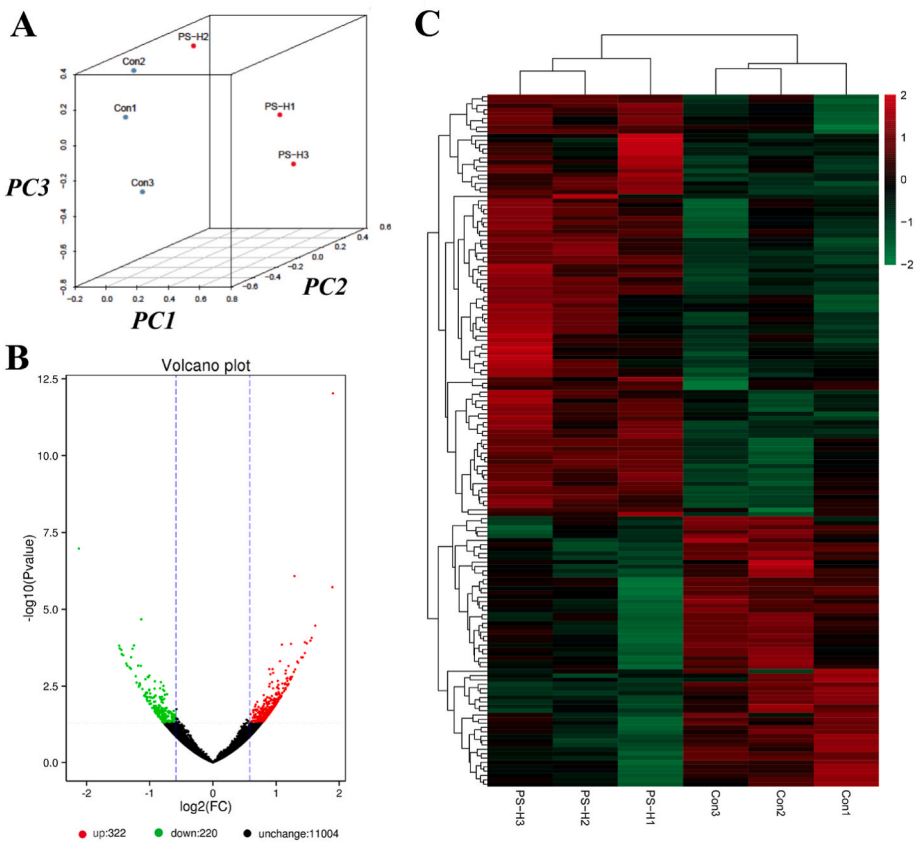

Fig. 4. Characterization of the transcriptome dataset. Principal component analysis (PCA) exhibits clear distinctions between control and PS-H groups (**A**). Heatmap of DEGs between control and PS-H groups (**B**). Volcano map of DEGs in digestive glands (q-value $\leq$ 0.05) (**C**).

maintenance of cellular homeostasis of *A. fangsiao* (Tamma et al., 2018). Similarly, the alteration of aquaporin gene supported the result of oxidative damage in the digestive gland cells of *A. fangsiao* caused by MPS exposure.

DEGs associated with DNA damage (Spindle and kinetochore associated protein 1, SKA1; Cyclin B) were found in this study. And KEGG pathways involved in DNA damage also exhibited significant enrichment, including base excision repair, nucleotide excision repair, DNA replication and mismatch repair. This result indicated that MPS exposure has induced DNA damage and triggered the responding mechanism of damage repair through transcriptional regulation and post-transcriptional regulation.

In addition, according to DEGs associated with transmembrane transport (such as Zinc transporter) and the considerable enrichment of the ABC transporters pathway in this study, MPS exposure also shows an adverse influence on transmembrane transport of digestive gland cells.

3.5. Effects of MPS exposure on metabolic profile

Subsequently, the above results led to an analysis of the possible metabolic disorders in the digestive gland based on metabolomic analysis. OPLS-DA model revealed significant separations between control and PS-H groups, indicating that MPS exposure has caused a remarkable metabolic difference in *A. fangsiao* digestive gland (Fig. 6A). The heatmap was also constructed to illustrate the variations of all metabolites between the two groups (Fig. 6B). As shown in Figs. 6C and 209 differential metabolites were observed between the control group and treated group, of which 104 metabolites were upregulated and 105 metabolites were downregulated in the high concentration of MPS exposure. Differential metabolites related to glycolipid metabolism (such as glucosyl passiflorate, phosphorylcholine (PC), O-Phosphoethanolamine (O-PEA) and LysoPC), oxidative stress (such as 1,3-Diaminopropane, Ranolazine and 4-Pyridoxic acid) and DNA damage (such as

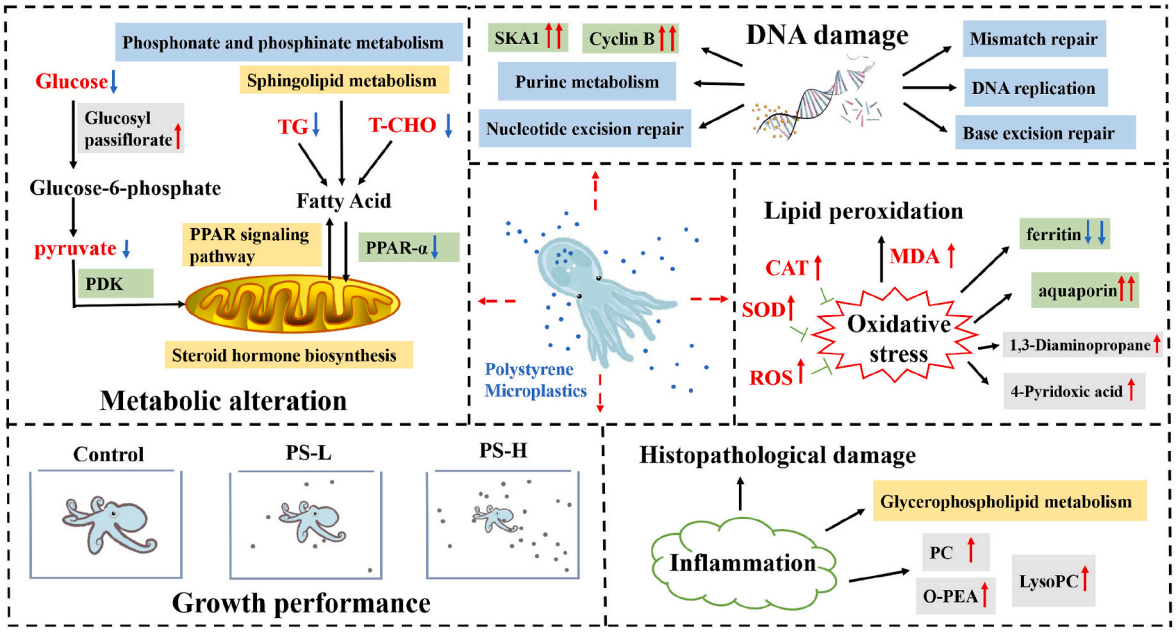

Fig. 5. Schematic representing biological pathways of cellular events in response to MPS exposure in *A. fangsiao*. The green box indicates the differential expression genes. The gray box indicates the differential metabolites. The blue box indicates DEGs based on transcriptomic analysis. The blue box indicates the KEGG pathway based on transcriptomic analysis. The yellow box indicates the KEGG pathway based on metabolomic analysis. The red font indicates biomarkers. The arrows indicate the regulation of biomarkers and metabolites. (For interpretation of the references to color in this figure legend, the reader is referred to the Web version of this article.)

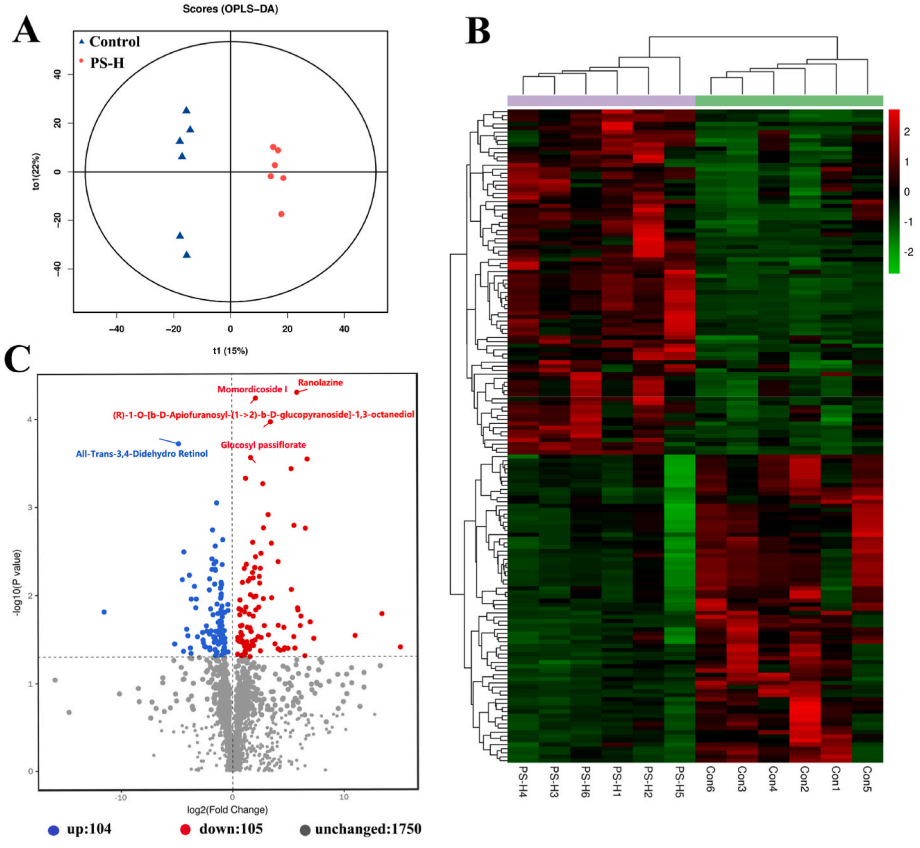

Fig. 6. Characterization of the metabolomic dataset. OPLS-DA analysis showing clear distinctions (**A**). Heatmap revealing the differential metabolites (**B**). Volcano map indicating the number of differential metabolites in digestive glands (q-value ≤ 0.05) (**C**).

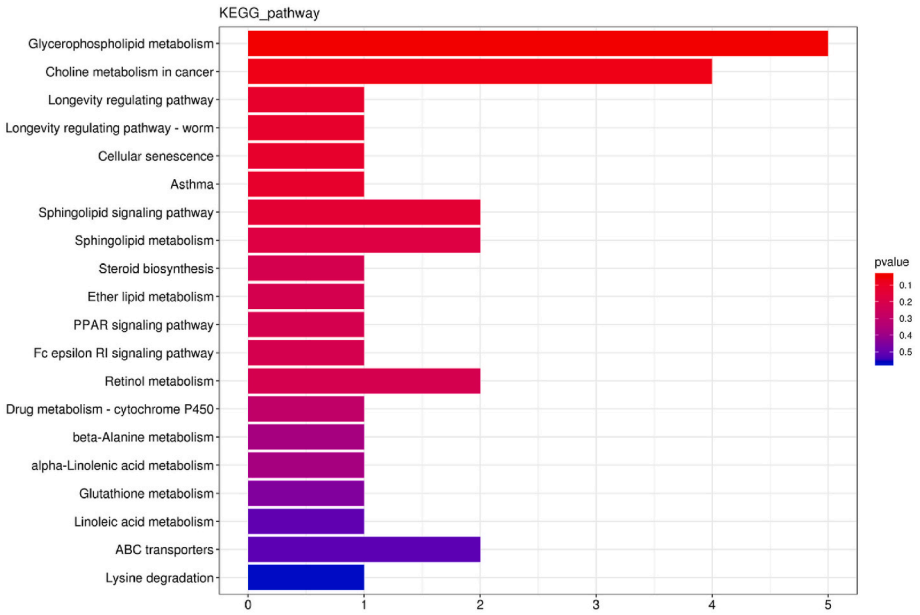

Fig. 7. Several crucial KEGG pathways in response to MPS stress in *A. fangsiao* based on metabolomic analysis (q-value < 0.05).

momordicoside) were found, which supported the above results.

To illustrate the primary influential metabolic pathways under MPS exposure, the analysis of KEGG enrichment was carried out (Fig. 7). The top 20 pathways were illustrated based on the data of pathway analysis. These pathways were mainly involved in glucolipid metabolism (PPAR signaling pathway and steroid hormone biosynthesis) and inflammation (glycerophospholipid metabolism).

The results of biochemical indicators and transcriptomic analysis have shown that MPS exposure has caused digestive gland glucose and lipid metabolism disorder. There, metabolomic analysis has proved these results. As described above, the enrichment of the PPAR signaling pathway in metabolomic analysis provided evidence to support the disorder of lipid metabolism in *A. fangsiao* digestive glands (Nguyen et al., 2008). Besides, steroid hormone biosynthesis and sphingolipid metabolism were considerably enriched in the present study, also proving the strong affection of MPS stress upon the lipid metabolism of *A. fangsiao* (Zhao et al., 2020).

The pathways related to inflammation were also enriched in the metabolomic analysis. The glycerophospholipid metabolism pathway was confirmed in the metabolomic analysis. As the cell membranes structural components, glycerophospholipids play an important role. Many differential metabolites involved in glycerophospholipid metabolism, including PC, O-PEA and LysoPC were detected in this study. Growing evidence has shown that PC can release a pro-inflammatory fatty acid called arachidonic acid (Kabarowski, 2009), which is an etiological factor in certain chronic inflammatory diseases (Teng et al., 2021a). The elevated levels of the PC in the PS-H groups revealed the inflammatory response of *A. fangsiao* under MPS exposure, which supported the results of histopathological analysis.

4. Conclusion

In this study, the growth performance, digestive gland histopathological analysis, oxidative stress biomarkers, metabolomic and transcriptomic profiles of *A. fangsiao* provide insight into the response of toxicity mechanism and detoxification under different MPS concentrations. It was found that the ingestion of MPS triggered several adverse effects, including growth restriction, histopathological damage, oxidative stress and metabolic disorders. For the detoxification mechanism against oxidative damage, *A. fangsiao* initiates an antioxidant response such as SOD and CAT with increasing levels of ROS and lipid peroxidation. Furthermore, the expression quantity of many metabolites and genes involved in DNA damage, oxidative stress, glucolipid metabolism, and inflammation have been altered to cope with the toxic effects of microplastic exposure. These results provide basic data for risk assessment of MPS exposure on the octopus and offered a good reference for ecotoxicology work.

Funding

We acknowledge grant support from the National Natural Science Foundation of China (32170536).

Credit author statement

Jian Zheng and Xiaodong Zheng conceived and designed the experiments; Jian Zheng and Congjun Li performed the experiments; Jian Zheng analyzed the data; Jian Zheng and Xiaodong Zheng contributed materials tools; Jian Zheng, Congjun Li and Xiaodong Zheng wrote the paper.

Declaration of competing interest

The authors declare that they have no known competing financial interests or personal relationships that could have appeared to influence the work reported in this paper.

Data availability

Data will be made available on request.

Appendix A. Supplementary data

Supplementary data to this article can be found online at https://doi.org/10.1016/j.envpol.2022.120480.

References

Avio, C.G., Gorbi, S., Milan, M., Benedetti, M., Fattorini, D., d Errico, G., Pauletto, M., Bargelloni, L., Regoli, F., 2015a. Pollutants bioavailability and toxicological risk from microplastics to marine mussels. Environ. Pollut. 198, 211e222.

Avio, C.G., Gorbi, S., Regoli, F., 2015b. Experimental development of a new protocol for extraction and characterization of microplastics in fish tissues: first observations in commercial species from Adriatic Sea. Mar. Environ. Res. 111, 18e26.
Bienert, G.P., Møller, A.L., Kristiansen, K.A., Schulz, A., Møller, I.M., Schjoerring, J.K., Jahn, T.P., 2007. Specific aquaporins facilitate the diffusion of hydrogen peroxide across membranes. J. Biol. Chem. 282 (2), 1183–1192.
Brandts, I., Barría, C., Martins, M.A., Franco-Martínez, L., Barreto, A., Tvarijonaviciute, A., Tort, L., Oliveira, M., Teles, M., 2021. Waterborne exposure of gilthead seabream (*Sparus aurata*) to polymethylmethacrylate nanoplastics causes effects at cellular and molecular levels. J. Hazard Mater. 403, 123590.
Browne, M.A., Dissanayake, A., Galloway, T.S., Lowe, D.M., ThoPSon, R.C., 2008. Ingested microscopic plastic translocates to the circulatory system of the mussel, Mytilus edulis (L). Environ. Sci. Technol. 42, 5026–5031.
Bu, D., Luo, H., Huo, P., Wang, Z., Zhang, S., He, Z., Wu, Y., Zhao, L., Liu, J., Guo, J., Fang, S., Cao, W., Yi, L., Zhao, Y., Kong, L., 2021. KOBAS-i: intelligent prioritization and exploratory visualization of biological functions for gene enrichment analysis. Nucleic Acids Res. 49 (W1), W317–W325.
Chen, S., Zhou, Y., Chen, Y., Gu, J., 2018. Fastp: an ultra-fast all-in-one FASTQ preprocessor. Bioinf 34, i884–i890, 2018.
Chen, Q., Lv, W., Jiao, Y., Liu, Z., Li, Y., Cai, M., Wu, D., Zhou, W., Zhao, Y., 2020. Effects of exposure to waterborne polystyrene microspheres on lipid metabolism in the hepatopancreas of juvenile redclaw crayfish. Cherax quadricarinatus. Aquat. Toxicol. 224, 105497.
Cole, M., Galloway, T.S., 2015. Ingestion of nanoplastics and microplastics by pacific oyster larvae. Environ. Sci. Technol. 49, 14625–14632.
Conesa, A., Götz, S., García-Gómez, J.M., Terol, J., Talon, M., Robles, M., 2005. Blast2GO: a universal tool for annotation, visualization and analysis in functional genomics research. Bioinf 21, 3674–3676.
Ding, J.N., Zhang, S.S., Razanajatovo, R.M., Zou, H., Zhu, W.B., 2018. Accumulation, tissue distribution, and biochemical effects of polystyrene microplastics in the freshwater fish red tilapia (Oreochromis niloticus). Environ. Pollut. 238, 1–9.
Eerkes-Medrano, D., Thompson, R.C., Aldridge, D.C., 2015. Microplastics in freshwater systems: a review of the emerging threats, identification of knowledge gaps and prioritisation of research needs. Water Res. 75, 63–82.
Eo, S., Hong, S.H., Song, Y.K., Lee, J., Lee, J., Shim, W.J., 2018. Abundance, composition, and distribution of microplastics larger than 20 μm in sand beaches of South Korea. Environ. Pollut. 238, 894–902.
Feng, Z.H., Zhang, T., Li, Y., He, X.R., Wang, R., Xu, J.T., Gao, G., 2019. The accumulation of Microplastics in fish from an important fish farm and mariculture area, Huizhou Bay. China Sci. Total Environ. 696, 133948.
Ferreira, G.V.B., Justino, A.K.S., Eduardo, L.N., 2022. Plastic in the inferno: microplastic contamination in deep-sea cephalopods(*Vampyroteuthis infernalis* and *Abralia veranyi*) from the southwestern Atlantic. Mar. Pollut. Bull. 174, 112209.
Filimonova, V., Goncalves, F., Marques, J.C., De Troch, M., Goncalves, A.M., 2016. Biochemical and toxicological effects of organic (herbicide Primextra Gold TZ) and inorganic (copper) compounds on zooplankton and phytoplankton species. Aquat. Toxicol. 177, 33e43.
Gao, F., Li, J., Hu, J., Sui, B., Wang, C., Sun, C., Li, X., Ju, P., 2021. The seasonal distribution characteristics of microplastics on bathing beaches along the coast of Qingdao, China. Sci. Total Environ. 783, 146969.
Gong, Y., Wang, Y., Chen, L., Li, Y., Liu, B., 2021. Microplastics in different tissues of a pelagic squid (*Dosidicus gigas*) in the northern Humboldt current ecosystem. Mar. Pollut. Bull. 169, 112509. Mar. Pollut. Bull. 169, 112509.
Ibáñez, C.M., Díaz-Santana-Iturrios, M., Carrasco, S.A., Fernández-Álvarez, F.A., López-Córdova, D.A., Cornejo, C.F., Ortiz, N., Rocha, F., Vidal, E.A.G., Pardo-Gandarillas, M.C., 2021. Macroevolutionary trade-offs and trends in life history traits of cephalopods through a comparative phylogenetic approach. Front. Mar. Sci. 8, 707825.
Jabeen, K., Li, B., Chen, Q., Su, L., Wu, C., Hollert, H., Shi, H., 2018. Effects of virgin microplastics on goldfish (*Carassius auratus*). Chemosphere 213, 323–332.
Janajreh, I., Alshrah, M., Zamzarn, S., 2015. Mechanical recycling of PVC plastic waste streams from cable industry: a case study. Sustain. Cities Soc. 18, 13e20.
Jiang, D.H., Zhen, X.D., Qian, Y.S., Zhang, Q.Q., 2020. Development of Amphioctopus fangsiao (Mollusca: cephalopoda) from eggs to hatchlings: indications for the embryonic developmental management. Mar. Life. Sci. Tech. 2 (1), 24–30.
Kabarowski, J.H., 2009. G2A and LPC: regulatory functions in immunity. Prostag. Other Lipid Mediat. 89 (3e4), 73e81.
Kanehisa, M., Araki, M., Goto, S., Hattori, M., Hirakawa, M., Itoh, M., Katayama, T., Kawashima, S., Okuda, S., Tokimatsu, T., 2007. KEGG for linking genomes to life and the environment. Nucleic Acids Res. 36, D480–D484.
Kim, D., Langmead, B., Salzberg, S.L., 2015. HISAT: a fast spliced aligner with low memory requirements. Nat. met. 12 (4), 357–360.
Kuhn, S., van Franeker, J.A., 2020. Quantitative overview of marine debris ingested by marine megafauna. Mar. Pollut. Bull. 151, 110858.
Li, C.J., Song, L.L., Zhou, Y., Yuan, J.S., Zhang, S.C., 2022. Identification of Isthmin1 in the small annual fish, *Nothobranchius guentheri*, as a novel biomarker of aging and its potential rejuvenation activity. Biogerontology 23 (1), 99–114. https://doi.org/10.1007/s10522-021-09948-5.
Lin, T., Yu, S., Chen, Y., Chen, W., 2014. Integrated biomarker responses in zebrafish exposed to sulfonamides. Environ. Toxicol. Pharmacol. 38 (2), 444–452.
Lindgren, A.R., Giribet, G., Nishiguchi, M.K., 2004. A combined approach of the phylogeny of Cephalopoda (Mollusca). Cladistics 20, 454–486.
Liu, Z., Yu, P., Cai, M., Wu, D., Zhang, M., Huang, Y., Zhao, Y., 2019. Polystyrene nanoplastic exposure induces immobilization, reproduction, and stress defense in the freshwater cladoceran Daphnia pulex. Chemosphere 215, 74–81.
Love, M.I., Huber, W., Anders, S., 2014. Moderated estimation of fold change and dispersion for RNA-seq data with DESeq2. Genome Biol. 15, 550.
Lu, C.C., 2000. Preliminary checklist of the cephalopods of the South China sea. Raffles Bull. Zool. 8, 539–567.
Lu, Y., Zhang, Y., Deng, Y., Jiang, W., Zhao, Y., Geng, J., Ding, L., Ren, H., 2016. Uptake and accumulation of polystyrene microplastics in zebrafish (Danio rerio) and toxic effects in liver. Environ. Sci. Technol. 50 (7), 4054–4060.
Lucia, M., André, J.M., Gonzalez, P., Baudrimont, M., Bernadet, M.D., Gontier, K., Maury Brachet, R., Guy, G., Davail, S., 2010. Effect of dietary cadmium on lipid metabolism and storage of aquatic bird *Cairina moschata*. Ecotoxicol 19, 163.
Mangold, K., 1983. *Octopus vulgaris*. In: Boyle, P. (Ed.), Cephalopod Life Cycles, Species Accounts, vol. I. Academic Press, United Kingdom. 335–364.
Martínez-Pita, I., Smanchez-Lazo, C., Ruíz-Jarabo, I., Herrera, M., Mancera, J.M., 2012. Biochemical composition, lipid classes, fatty acids and sexual hormones in the mussel *Mytilus galloprovincialis* from cultivated populations in south Spain. Aquacult 358, 274e283.
Mishra, A.K., Singh, J., Mishra, P.P., 2021. Microplastics in polar regions: an early warning to the world's pristine ecosystem. Sci. Total Environ. 784, 147149.
Nguyen, P., Leray, V., Diez, M., Serisier, S., Le Bloc'h, J., Siliart, B., 2008. Liver lipid metabolism. J. Anim. Physiol. Anim. Nutr. 92, 272–283.
Okutan, H., Ozcelik, H.R., Yilmaz, U.E., 2005. Effects of caffeic acid phenethyl ester on lipid peroxidation and antioxidant enzymes in diabetic rat heart. Clin. Biochem. 38 (2), 191–196.
Oliveira, A.R., Sardinha-Silva, A., Andrews, P.L.R., Green, D., Cooke, G.M., Hall, S., Blackburn, K., Sykes, A.V., 2020. Microplastics presence in cultured and wild-caught cuttlefish, *Sepia officinalis*. Mar. Pollut. Bull. 160, 111553.
Pan, Y.B., Zhang, W.J., Lin, S.J., 2018. Transcriptomic and micrornaomic profiling reveals molecular mechanisms to cope with silver nanoparticle exposure in the ciliate *Euplotes vannus*. Environ Sci-Nano 5 (12), 2921–2935.
Paul-Pont, I., Lacroix, C., González, Fernández, C., Hégaret, H., Lambert, C., Le Goïc, N., Frère, L., Cassone, A.L., Sussarellu, R., Fabioux, C., Guyomarch, J., Albentosa, M., Huvet, A., Soudant, P., 2016. Exposure of marine mussels Mytilus spp. to polystyrene microplastics: toxicity and influence on fluoranthene bioaccumulation. Environ. Pollut. 216, 724–737.
Peda, C., Longo, F., Berti, C., Laface, F., De Domenico, F., Consoli, P., Battaglia, P., Greco, S., Greco, Y., 2022. The waste collector: information from a pilot study on the interaction between the common octopus (*Octopus vulgaris*, Cuvier, 1797) and marine litter in bottom traps fishing and first evidence of plastic ingestion. Mar. Pollut. Bull. 174, 113185.
Peters, C.A., Bratton, S.P., 2016. Urbanization is a major influence on microplastic ingestion by sunfish in the Brazos River basin, Central Texas, USA. Environ. Pollut. 210, 380–387.
Plastics Europe, 2022. Plastics-The Facts. An Analysis of European Plastics Production, Demand and Waste Data, p. 12.
Prato, E., Danieli, A., Maffia, M., Biandolino, F., 2010. Lipid and fatty acid compositions of *Mytilus galloprovincialis* cultured in the mar grande of taranto (southern Italy): feeding strategies and trophic relationships. Zool. Stud. 49 (2), 211–219.
Qiao, R., Sheng, C., Lu, Y., Zhang, Y., Ren, H., Lemos, B., 2019. Microplastics induce intestinal inflammation, oxidative stress, and disorders of metabolome and microbiome in zebrafish. Sci. Total Environ. 662, 246–253.
Rochman, C.M., Kurobe, T., Flores, I., The, S.J., 2014. Early warning signs of endocrine disruption in adult fish from the ingestion of polyethylene with and without sorbed chemical pollutants from the marine environment. Sci. Total Environ. 493, 656–661.
Sanchez, W., Burgeot, T., Porcher, J.M., 2013. A novel 'integrated biomarker response' calculation based on reference deviation concept. Environ. Sci. Pollut. Res. 20 (5), 2721–2725.
Sussarellu, R., Suquet, M., Thomas, Y., Lambert, C., Fabioux, C., Pernet, M.E., Le, GoïcN., Quillien, V., Mingant, C., Epelboin, Y., Corporeau, C., Guyomarch, J., Robbens, J., Paul-Pont, I., Soudant, P., Huvet, A., 2016. Oyster reproduction is affected by exposure to polystyrene microplastics. Proc. Natl. Acad. Sci. U.S.A. 113 (9), 2430–2435.
Tamma, G., Valenti, G., Grossini, E., Donnini, S., Marino, A., Marinelli, R.A., Calamita, G., 2018. Aquaporin membrane channels in oxidative stress, cell signaling, and aging: recent advances and research trends. Oxid. Med. Cell. Longev., 1501847
Teng, J., Zhao, J., Zhu, X., Shan, E., Zhang, C., Zhang, W., Wang, Q., 2021a. Toxic effects of exposure to microplastics with environmentally relevant shapes and concentrations: accumulation, energy metabolism and tissue damage in oyster *Crassostrea gigas*. Environ. Pollut. 269, 116169.
Teng, J., Zhao, J.M., Zhu, X.P., Shan, E.C., Wang, Q., 2021b. Oxidative stress biomarkers, physiological responses and proteomic profiling in oyster (*Crassostrea gigas*) exposed to microplastics with irregular-shaped PE and PET microplastic. Sci. Total Environ. 786, 147725.
Tisma, V.S., Basta-Juzbasic, A., Jaganjac, M., Brcic, L., Dobric, I., Lipozencic, J., Tatzber, F., Zarkovic, N., Poljak-Blazi, M., 2009. Oxidative stress and ferritin expression in the skin of patients with rosacea. J. Am. Acad. Dermatol. 60 (2), 270–276.
Vidal, E., Villanueva, R., Andrade, J.P., Gleadall, I.G., Wood, J., 2014. Cephalopod culture: current status of main biological models, and research priorities. In: vidal, E. A.G. (Ed.), Advances in Cephalopod Science, Biology, Ecology, Cultivation and Fisheries. Adv. Mar. Biol., vol. 67, pp. 1–98.
Wan, Z., Wang, C., Zhou, J., Shen, M., Wang, X., Fu, Z., Jin, Y., 2019. Effects of polystyrene microplastics on the composition of the microbiome and metabolism in larval zebrafish. Chemosphere 217, 646–658.
Wang, W., Dong, G., Yang, J.M., Zheng, X.D., Wei, X., Sun, G., 2015. The development process and seasonal changes of the gonad in *Octopus ocellatus* gray off the coast of qingdao, northeast China. Fish. Sci. 81, 309–319.

Weber, A., Scherer, C., Brennholt, N., Reifferscheid, G., Wagner, M., 2018. PET microplastics do not negatively affect the survival, development, metabolism and feeding activity of the freshwater invertebrate *Gammarus pulex*. Environ. Pollut. 234, 181–189.

Xiang, K.Y., He, Z., Fu, J., Wang, G., Li, H., Zhang, Y., Zhang, S.C., Chen, L., 2022. Microplastics exposure as an emerging threat to ancient lineage: a contaminant of concern for abnormal bending of amphioxus via neurotoxicity. J. Hazard Mater. 438, 129454.

Xu, F.S., 2008. Class cephalopoda. In: Liu, R.Y. (Ed.), Checklist of Marine Biota of China Seas. Science Press, Beijing, pp. 598–606.

Xu, S., Ma, J., Ji, R., Pan, K., Miao, A.J., 2020. Microplastics in aquatic environments: occurrence, accumulation, and biological effects. Sci. Total Environ. 703, 134699, 9.

Yang, J., Lee, S.H., Goddard, M.E., Visscher, P.M., 2011. Gcta: a tool for genome-wide complex trait analysis. Am. J. Hum. Genet. 88, 76–82.

Zhao, Y., Bao, Z., Wan, Z., Fu, Z., Jin, Y., 2020. Polystyrene microplastic exposure disturbs hepatic glycolipid metabolism at the physiological, biochemical, and transcriptomic levels in adult zebrafish. Sci. Total Environ. 710, 136279.

Zhao, X., Sun, Z.C., Gao, T.X., Song, N., 2021. Transcriptome profiling reveals a divergent adaptive response to hyper- and hypo-salinity in the yellow drum, *Nibea albiflora*. Animals (London) 11 (8).

Zheng, J., Zhao, L., Zhao, X., Gao, T., Song, N., 2022. High genetic connectivity inferred from whole-genome resequencing provides insight into the phylogeographic pattern of *Larimichthys polyactis*. Mar. Biotechnol. 24 (4), 671–680. https://doi.org/10.1007/s10126-022-10134-y.